

Research on Non-line-of-sight Positioning Method of Smart Mobile Terminal Based on Acoustic Signal in Wireless Sensing Room

Jianjun Liu^{1,*} and Yue Jin²

¹School of Information Science and Engineering, Hebei North University, Zhangjiakou, Hebei, China, 000730

²School of Electrical Engineering, Zhangjiakou Vocational and Technical College, Zhangjiakou, Hebei, China, 000730

Article Info

Volume 83

Page Number: 5546 - 5552

Publication Issue:

July - August 2020

Article History

Article Received: 25 April 2020

Revised: 29 May 2020

Accepted: 20 June 2020

Publication: 28 August 2020

Abstract

The technology in the research of the non-line-of-sight positioning method for smart mobile terminals based on acoustic signals in the wireless sensing room effectively solves the test of non-line-of-sight positioning, which traditional sensors cannot solve. The successful development of the non-line-of-sight positioning method of smart mobile terminals based on acoustic signals in wireless sensing rooms has realized the indoor and outdoor non-distance positioning of smart mobile terminals.

Keywords: Intelligent Mobile Terminal of Acoustic Signal, Non-line-of-sight Positioning, Wireless Sensing Room;

1. Introduction

With the development of the Internet, many smart mobile devices require intelligent terminals with acoustic signals, such as navigation, positioning, etc., and the real data will always have corresponding errors due to the unstable factors of the sensors^[1-3]. Foreign countries have long studied passive acoustic detection technology, but there are few non-line-of-sight positioning in existing research^[4-6]. This paper proposes a non-line-of-sight positioning method for smart mobile terminals based on wireless sensors, and establishes a linear model through acoustic signals to achieve improved positioning.

2. Basic principles

2.1. Positioning model

In the actual non-line-of-sight acoustic localization environment, the main obstacles are generally hills and mountains with slow undulation, which determines that the acoustic signal generally propagates to the base array through direct or diffraction. Introduce the following assumptions:

(1) The sound source is a point sound source and is far away from the receiving array;

(2) The signal propagation from the target to the base array in the model is simply divided into three segments: direct-diffraction-direct, that is, the

acoustic signal reaches the obstacle in a direct way, and then the propagation mode on the surface of the obstacle is diffraction until it leaves. After the obstacle, shoot directly to the base array;

(3) The coordinates of each point on the base array and obstacle surface in the model are known, and there are multiple base arrays to measure the AOA value of the acoustic signal.

The model is shown in Figure 1.

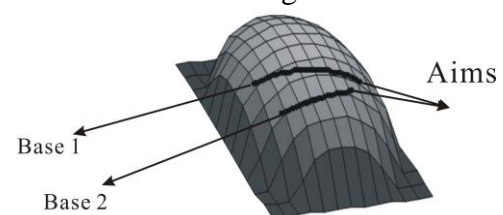


Figure 1. Ray tracing positioning model.

2.2. Principle of diffraction

In the model in Figure 1, the presence of obstacles makes the acoustic signal reach the base array only through diffraction. Due to the effect of the obstacle surface, the sound wave will continuously leak (radiate) energy along the tangent direction of the surface during the diffraction and propagation process, and propagate close to the surface. Physically, the wave transmitted in this way is called a creeping wave. Or creeping waves. When the crawling wave travels along the curved surface, it

follows the generalized Fermat principle: the propagation path is a short-range line, that is, the path that the crawling wave travels between two points on the curved surface is the path with the smallest length value among all possible paths. Geodesic has the following properties:

- (1) Starting from every point on the surface, to any other point, there is always a unique geodesic;
- (2) The necessary condition for a curve Γ to be a geodesic on a curved surface is that Γ is a straight line, or the tangent plane of Γ (the plane formed by the tangent and the secondary normal is called the secondary tangent, and the secondary normal is the normal and the tangent. The vector of intersection) coincides with the tangent surface of the surface;
- (3) On a curved surface, among all curves with the same tangent at the same point, the curvature of the geodesic is the smallest, and the curvature of the geodesic is the normal section of the same direction (the intersection of the normal plane of a certain point on the surface and the surface Called normal section) curvature.

The propagation path of the signal on the curved surface can be obtained by solving the geodesic. If the surface is relatively simple, ray tracing can be performed by solving analytical geometric equations or second-order differential equations, but most arbitrary surfaces cannot be analytically solved. In this paper, the geodesic of the diffraction part is approximated by a series of discrete points, and then the ray tracing is carried out through the iterative relationship between points.

A three-dimensional coordinate system is established on the curved surface, and the schematic diagram of ray tracking is shown in Figure 2.

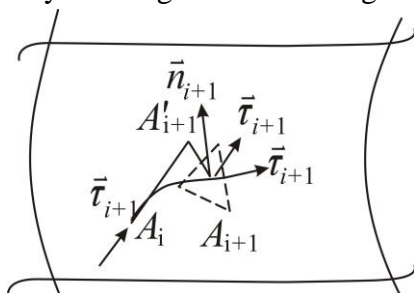


Figure 2. Schematic diagram of ray tracing.

Suppose the coordinates of a point A_i on the geodesic line are (x_i, y_i, z_i) , and the unit vector $\vec{\tau}_i$ of the incident direction of the acoustic signal at the point A_i is $(\alpha_i, \beta_i, \gamma_i)$. Assuming that the acoustic signal propagates in a straight line from point A_i to point A'_{i+1} in the $\vec{\tau}_i$ direction, the x coordinate value increases by h , because point A_i and point A'_{i+1} are both on the straight line with the direction τ_i , it is easy to deduce point A'_{i+1} . The increase in the y coordinate of $+1$ is $h\alpha_i/\beta_i$. Assuming that when the acoustic signal propagates along the geodesic line to the next point A_{i+1} , the xy coordinate of the point A_{i+1} is equal to the xy coordinate of the point A'_{i+1} , and the obtained xy coordinate value is substituted into the geographic information system to obtain the point A_{i+1} . The corresponding z coordinate, set its value to z_{i+1} . Then the coordinates of point A_{i+1} on the geodesic line are:

$$A_{i+1} = \left(x_i + h, y_i + h \frac{\alpha_i}{\beta_i}, z_{i+1} \right) \quad (1)$$

From the geographic information of the small area near A_{i+1} point, the normal vector \vec{n}_{i+1} of the surface at A_{i+1} point can be calculated (in this simulation experiment, any three points with A_{i+1} point distance less than h are taken to obtain a small triangular area. Geographical information can know the coordinates of these three points, and the normal vector of the plane determined by these three points is used as the normal vector of the surface at A_{i+1}), and G is any point on the plane, and the point A_{i+1} can be determined. The point normal vector equation of the tangent plane $Q1$ is:

$$\vec{n}_{i+1} \circ (G - A_{i+1}) = 0 \quad (2)$$

Translate the unit vector $\vec{\tau}_i$ to A_{i+1} , the plane $Q2$ determined by A_{i+1} , $\vec{\tau}_i$ and \vec{n}_{i+1} is:

$$(\vec{n}_{i+1} \times \vec{\tau}_i) \circ (G - A_{i+1}) = 0 \quad (3)$$

According to the properties of the geodesic proposed in the previous section, the direction of the

intersection line L of Q1 and Q2 is the direction of the geodesic at point A. Because the line of intersection L is perpendicular to the normal vector of Q and Q2, it is also perpendicular to the plane determined by the normal vector of planes Q1 and Q2. Therefore, the direction of the intersection, that is, the direction vector of the signal propagating at Ai+1 is:

$$\vec{\tau}_{i+1} = \vec{n}_{i+1} \times \vec{\tau}_i \times \vec{n}_{i+1} \quad (4)$$

After setting the value of the initial point, iterate according to equations (1) and (4) to obtain the coordinates and ray directions of all discrete points on the geodesic line of signal propagation with an interval of h.

Suppose a total of two base matrices are involved in positioning, and the j-th discrete point of base matrix 1 and the k-th discrete point of base matrix 2 are arbitrarily taken, and the coordinate and acoustic signal direction vectors at these two points are Aj, $\vec{\tau}_j$ and Ak, $\vec{\tau}_k$. The straight lines Lj and Lk that have made discrete points and whose directions are the direction vectors to be sought, the parametric equations with s and t as parameters are:

$$\begin{cases} L_j(s) = A_j + s\vec{\tau}_j \\ L_k(t) = A_k + t\vec{\tau}_k \end{cases} \quad (5)$$

Ideally, when two straight lines intersect at a point, the intersection point is considered to be a location estimate point. However, due to the calculation accuracy of the computer, the approximate value in the iterative algorithm, and the error of the measured value, the two lines generally do not intersect strictly. Assuming that the distance between the point Pj on Lj and the point Pk on Lk is the minimum distance between the two straight lines, when the minimum distance is less than the fixed threshold g, it is considered that this set of discrete points can obtain an estimated value point, and Let the estimated value point be the midpoint of the connection between Pj and Pk

3. System Model

3.1. Inertial sensor alignment

Compared with its own sensor, when the wireless sensor room is based on robot navigation, the direction of the inertial sensor relative to the robot is unknown, so the inertial sensor of the smart terminal needs to be aligned, that is, the yaw angle, pitch angle and roll of the smart terminal gyroscope are measured. Angle. Pitch angle and roll angle are based on the measurement of gravitational acceleration relative to the world, and the yaw angle is the measurement of relative terminal position. Since the position of the intelligent terminal on the robot is unknown, this article uses the automatic alignment method in the literature to obtain the intelligent terminal Relative to the robot's yaw angle γ_{S-V} , the yaw angle obtained from a single sampling is

$$\gamma_{S-V} = \begin{cases} \arcsin\left(\frac{a_{z_V}}{|a_{y_{z_V}}|}\right), a_{y_{KF}} \geq 0 \\ \pi - \arcsin\left(\frac{a_{z_V}}{|a_{y_{z_V}}|}\right), other \end{cases} \quad (6)$$

Where: azV is the z-axis acceleration; ayzV is the composite acceleration of the y-axis and z-axis; ayKF is the acceleration of the y-axis after Kalman filtering, and

$$|a_{y_{z_V}}| = \sqrt{|a_{y_V}|^2 + |a_{z_V}|^2}$$

Then, the terminal coordinate system and the robot coordinate system are projected to the world coordinate system (as shown in Figure 3), thereby establishing a dynamic model in the world coordinate system.

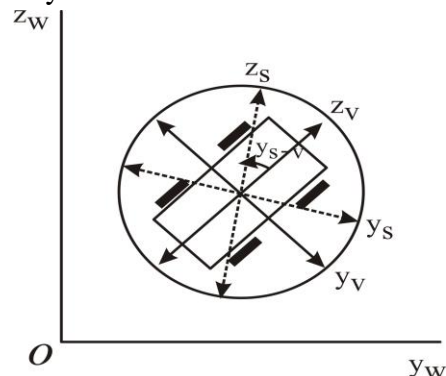


Figure 3. Robot motion model in the world coordinate system.

3.2. Acoustic signal acquisition of preliminary indoor position of smart mobile terminal

In this paper, the iBeacon wireless network is deployed indoors to determine the initial position of the robot, and then particle filtering is used to fuse inertial sensors for precise positioning. Due to the complex indoor environment and the iBeacon signal has a strong time-varying nature, the wireless signal attenuation model cannot accurately reflect The relationship between distance and received signal strength, and the matching and positioning method based on fingerprint database has good robustness. The matching and positioning algorithm of fingerprint database is mainly divided into two steps: ① Offline sampling. Measurements at each reference point come from different iBeacon The received signal strength, and the iBeacon data major and minor, longitude and latitude are stored in the fingerprint database; ②Online positioning. Use a suitable matching algorithm to match the signal strength vector received by iBeacon with the data in the fingerprint database to Seek the most similar data to obtain the estimated robot position. This paper uses the weighted nearest neighbor algorithm to find the target position of the robot.

3.3. State equation

The system state equation is established according to the robot motion model, and the state vector of the system at time k is

$$X_k = [p_k^e \quad p_k^n \quad v_k^e \quad v_k^n \quad \theta]^T \quad (7)$$

Where: p_k^e is the east position of the robot at time k; p_k^n is the north position of the robot at time k; v_k^e is the east speed of the robot at time k; v_k^n is the north speed of the robot at time k; θ is the observed track and the estimated track The angle between (DR). The discrete state equation is

$$X_{k+1} = AX_k + W_k \quad (8)$$

3.4. Observation equation

Taking the preliminary position information obtained by iBeacon and GPS as two sets of different observations, the observation equation of the obtained system is

$$Z_k = H_k X_k + G_k \quad (9)$$

$$Z_k = [p_k^{e'} \quad p_k^{n'} \quad v_k^{e'} \quad v_k^{n'}]^T \quad (10)$$

Considering that the observation noises of GPS and iBeacon are different during the traveling of the robot, two sets of observation white noise $G_k^i (i=1,2)$ are introduced, and the resulting model set is

$$\left. \begin{aligned} X_{k+1} &= AX_k + W_k \\ Z_k &= H_k X_k + G_k^i \end{aligned} \right\} \quad (11)$$

4. Fusion Algorithm

The Markov parameter adaptive interactive multi-model particle filter AMP-IMM-PF (Adaptating Markov Parameter-Interactive Multi Model-Particle Filter) algorithm structure diagram proposed in this paper is divided into input interaction, model matching filtering, and model probability. Update, estimate output and real-time correction of Markov transition probability in 5 parts.

4.1. Input interaction

The AMP-IMM-PF algorithm uses the second-order Markov chain as the basis for model switching, as shown in Figure 4. The model switching probability is

$$\left. \begin{aligned} u_k^{ij} &= (1/c_j) p_{ij} u_{k-1}^i \\ c_j &= \sum_i p_{ij} u_{k-1}^i \end{aligned} \right\} \quad (12)$$

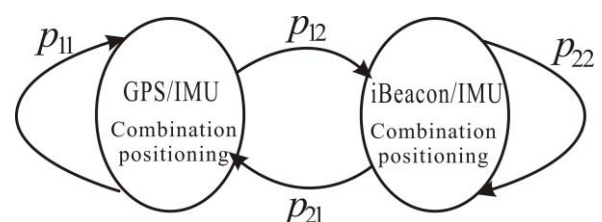


Figure 4. Markov chain.

Where: u_k^{ij} is the transition probability of model i input to model j at time k ; p_{ij} is the model transition probability of Markov chain, which represents the transition probability from model i to model j ; u_{k-1}^i is the transition probability of model i at time $k-1$ Model probability.

The calculated initial estimate of model j at time k is

$$X_k^{0j} = \sum_i X_{k-1}^{0i} u_k^{ij} \quad (13)$$

The initial covariance of model j at time $k-1$ is

$$S_{k-1}^{0j} = \sum_i u_{k-1}^{ij} \left\{ S_{k-1}^{0i} + [X_{k-1}^{0i} - X_{k-1}^{0j}] [X_{k-1}^{0i} - X_{k-1}^{0j}]^T \right\} \quad (14)$$

4.2. Model matched filtering

The fusion of GPS/IMU and iBeacon/IMU is a non-linear and non-Gauss problem. Therefore, this paper uses two different particle filters to filter the observation distance. The designed particle filter process is as follows:

(1) Particle initialization. Set up an initial sample set in the initial stage of particle filter positioning. Each particle in the set has a corresponding weight, which represents the possibility of the robot at the position of the particle. According to the position coordinates of the east and north directions Range, initialize M random particle samples, the initial weight q_i of particle i is set to $1/M$, namely

$$\left. \begin{aligned} x_i &= \text{rand}(x_{\min}, x_{\max}) \\ y_i &= \text{rand}(y_{\min}, y_{\max}) \\ q_i &= 1/M \\ i &= 1, 2, \dots, M \end{aligned} \right\} \quad (15)$$

In the formula, rand is an equal probability random value.

(2) Prediction stage. According to the robot motion model and combined with the data processing results of the IMU sensor, the system state equation is used to predict the position of the robot at the next moment.

First, make a decision. The particle weight is updated, and the particle weight updated at $k+1$ is

$$q_{k+1}^i = \frac{1}{\sqrt{2\pi R}} \exp \left[-\frac{(Z_k - X_k^i)^2}{2R} \right] \quad (16)$$

Where: q_{k+1}^i is the weight of particle i at $k+1$; R is the variance of the measurement noise.

Then, use the following formula to normalize the particle weights:

$$q_{k+1}^i = q_{k+1}^i / \sum_{j=1}^M q_{k+1}^j \quad (17)$$

Next is resampling. Resampling is the key to particle filtering. This article uses the posterior probability density $P(X_k|Z_k)$ to generate M new particles to solve the particle degradation problem, namely

$$P(X_k | Z_k) = \sum_{i=1}^M q_{k+1}^i \delta(X_k - X_{k-1}^i) \quad (18)$$

In the formula, $\delta(X_k - X_{k-1}^i)$ is the unit impulse function.

Finally, return to the particle prediction stage, enter the next cycle, and predict the state X_{k+1} at time $k+1$.

4.3. Model probability update

Assuming that the model likelihood is a Gaussian distribution, the residual V_k^{0j} and the residual covariance $S^j(k)$ of the j -th model observation value and the measured value under the action of M particles are used to calculate the model likelihood at time k , namely

$$\Delta_k^j = N(V_k^{0j}; 0, S^j(k)) \quad (19)$$

$S^j(k)$ can be obtained by the covariance of M particles, namely

$$S^j(k) = \sum_{i=1}^M [S_i^j(k)] [S_i^j(k)]^T \quad (20)$$

Then, use the following formula to update the

model probability:

$$\left. \begin{aligned} u_k^j &= (1/c) \Delta_k^j u_j \\ c &= \sum_j \Delta_k^j u_j \end{aligned} \right\} \quad (21)$$

Where: u_j is the model probability; Δ_k^j is the likelihood function of each observer at time k .

4.4. Estimated output

Using the estimated value output by the particle filter and the mean value of its covariance, the final robot position obtained by weighted fusion is

$$X_k = \sum_i X_k^i u_k^i \quad (22)$$

4.5. Real-time correction of model transition probability

When the robot is in the non-transition area, the accuracy loss caused by the competition of the mismatched model should be avoided; when the robot is in the transition area, the switching speed of the GPS and iBeacon observation models should be ensured, and the measurement information of the two should be fully utilized to improve the particle filter. Based on the traditional interactive multi-model particle filter (IMM-PF) algorithm, this paper uses the weighted power of the 2 model error compression ratios to modify the IMM-PF algorithm to meet the transition area and non-transition area. The requirements for the Markov state transition matrix and improve the tracking and positioning accuracy.

5. Results and analysis

In this paper, an iBeacon/IMU/GPS combined positioning system experimental platform is built on a robot equipped with an Apple tablet. The experimental site is located in Building 2, Qiyuan Science and Technology Park, Shanghai. 11 iBeacon beacons are deployed indoors, and the fingerprint points are separated by 5m. Among them, The light-colored line segment is the indoor path, and the dark-colored line segment is the outdoor path. The initial Markov transition probability matrix of the AMP-IMM-PF algorithm proposed in this paper is

set as

$$P = [0.95 \quad 0.05 \quad 0.05 \quad 0.95]$$

The initial probability of the model is set to 0.5, the initial input value of each model is set to the measured value, and the weighted power exponent $t=2.5$.

The iBeacon observation model using the AMP-IMM-PF algorithm is compared with the measured distance error and the cumulative probability distribution of the error obtained from the GPS observation model of the traditional IMM-PF algorithm. It can be seen that the measurement distance error of the iBeacon observation model is smaller, and the GPS is used. The error of the measurement distance obtained by the observation model is relatively large; after particle filtering, the errors of the iBeacon and GPS observation models are reduced, and the positioning accuracy of the entire system is improved. Figure 7(c) and (d) show IMM- The probability statistics results of the PF algorithm and the AMP-IMM-PF algorithm. It can be seen that the AMP-IMM-PF algorithm estimates the probability of the model very accurately. When the real situation is indoor ($t=0\sim 100s$), it is suitable for the indoor environment. The probability of the iBeacon observation model is greater than that of the GPS observation model. When the traditional IMM-PF algorithm is in a non-transition area, the model probability fluctuates more than the AMP-IMM-PF algorithm, which is caused by the competition of the introduction of mismatched models. The accuracy is reduced; and the Markov transition probability matrix of the AMP-IMM-PF algorithm in the transition area and the non-transition area can be adjusted adaptively, so that it has strong robustness and high in the transition area and the non-transition area. The tracking accuracy of the model and the dynamics of the model probability can produce a faster response to the observation model, so as to adapt to the scene of indoor and outdoor non-line-of-sight switching. It can be seen that the AMP-IMM-PF algorithm proposed in this paper has a good effect.

Table 1 lists the comparison results of the positioning error of the algorithm in this paper and other algorithms. It can be seen that the average error of the algorithm in this paper is small, and the cumulative probability of its error less than 10m is significantly higher than that of other algorithms. Other algorithms are in the order of ms.

Table 1. The positioning error of the algorithm in this paper and other methods.

Algorithm	Average error/m	Cumulative probability of error less than 10m/
AMP-IMM-PF	3.2	94
IMM-PF	3.7	92
PF-iBeacon	5.0	86
PF-GPS	5.2	93
IMM-EKF	5.9	81

6. Conclusion

In order to realize the indoor and outdoor non-line-of-sight positioning of the intelligent mobile terminal of the acoustic signal, this paper derives the robot motion model based on the intelligent terminal, and proposes the AMP-IMM-PF algorithm, and uses the intelligent terminal to construct the iBeacon/IMU/GPS combined positioning system. It shows that compared with the single-model algorithm, the proposed AMP-IMM-PF algorithm can reduce the positioning error in different environments and the linearization error of EKF; in the case of uncertain observation noise, the algorithm in this paper can automatically adjust System model to ensure rapid system convergence and improve positioning accuracy.

References

[1] Hammes, U., & Zoubir, A. M.. (2010). Robust mobile terminal tracking in nlos environments based on data association. *IEEE Transactions on Signal Processing*, 58(11), 5872-5882.

[2] Long, F., & Xu, H.. (2012). Research on signal analysis method of acoustic emission of material 2.25cr-1mo based on wavelet

filter and clustering. *Lecture Notes in Electrical Engineering*, 126, 821-827.

[3] Du, Y., Shi, W., & Liu, C.. (2012). Research on an efficient method of license plate location. *Physics Procedia*, 24, 1990-1995.

[4] Ahmed, & Ali, A.. (2015). A comparative study of qos performance for location based and corona based real-time routing protocol in mobile wireless sensor networks. *Wireless Networks*, 21(3), 1015-1031.

[5] Hu, M., Wang, J., Zhang, Y., Cai, C., & Wang, X.. (2012). Experimental research on volume measurement method of weights based on acoustic principle. *Yi Qi Yi Biao Xue Bao/Chinese Journal of entific Instrument*, 33(10), 2337-2342.

[6] Maiti, S., Mikami, M., & Hoshino, K.. (2017). Field experimental evaluation of mobile terminal velocity estimation based on doppler spread detection for mobility control in heterogeneous cellular networks. *ICE Transactions on Communications*, E100.B(2), 252-261